

# Scaling behavior in a quantum wire with scatterers

Daniel Boese

*Institut für Theoretische Festkörperphysik, Universität Karlsruhe, D-76128 Karlsruhe, Germany  
Forschungszentrum Karlsruhe, Institut für Nanotechnologie, D-76021 Karlsruhe, Germany*

Markus Lischka

*Physik-Department T30, Technische Universität München, D-85747 Garching, Germany*

L. E. Reichl

*Center for Studies in Statistical Mechanics and Complex Systems,  
The University of Texas at Austin, Austin, Texas 78712*

(November 2, 2018)

We study the conductance properties of a straight two-dimensional quantum wire with impurities modeled by  $s$ -like scatterers. Their presence can lead to strong inter-channel coupling. It was shown that such systems depend sensitively on the number of transverse modes included. Based on a poor man's scaling technique we include the effect of higher modes in a renormalized coupling constant. We therefore show that the low-energy behavior of the wire is dominated by only a few modes, which hence is a way to reduce the necessary computing power. The technique is successfully applied to the case of one and two  $s$ -like scatterers.

72.20-i,72.20.Jv,72.10.Fk

## I. INTRODUCTION

Over the past decade, quantum transport in two-dimensional electron systems has attracted increasing attention. In electron waveguide structures, the transmission and resonance phenomena have been studied extensively, especially because the conductance was shown to be directly related to the scattering properties of the system. This relation is known as Landauer-Büttiker formula,<sup>1-5</sup>

$$G = \frac{e^2}{h} T, \quad (1)$$

where  $G$  denotes the 2-point conductance and  $T$  the full transmission function (spin degrees of freedom are neglected). Eq. (1) results in a quantized conductance for ballistic channels, which has been experimentally verified for a large range of conduction channels.<sup>6</sup>

It is therefore of great interest to study the properties of ballistic wires containing impurities. Especially for attractive scatterers the combined effect of the scatterer itself and the backscattering off the walls leads to interesting phenomena such as resonances and quasi-bound states.<sup>7-12</sup> Moreover strong inter-channel coupling is introduced into the system making calculations quite complicated. A simple model containing all of the features mentioned above consists of a point-like scatterer modeled by a two-dimensional  $\delta$ -function.<sup>7-9</sup> In this paper we present a way to dramatically reduce the computational complexity of this problem by including the effect of the higher modes in a renormalized coupling constant.

The outline of this paper is as follows: In the next section we present the standard approach to calculating the conductance in this kind of waveguide setup. We

then briefly discuss results for two model systems for an impurity in the waveguide. For the case of a  $\delta$ -function impurity, we introduce a scaling approach and discuss the results for the rescaled system. We finally generalize the scaling approach to a system with many scatterers and show results for the case of two  $\delta$ -function scatterers.

## II. CONDUCTANCE CALCULATION

In this section we sketch the calculation of the conductance of an electron waveguide including a general scatterer. We restrict ourselves to a single scatterer, because the transmission matrix for many scatterers can be obtained by multiplying together the transmission matrices for the individual single scatterers.

Let us first obtain a solution of the Schrödinger equation for an electron in a two-dimensional waveguide with a general scatterer. The Hamiltonian is given by

$$H = \frac{p^2}{2m} + V(x, y) + V_c(y). \quad (2)$$

$V_c$  represents a confinement potential restricting the transverse movement of the electron and  $V(x, y)$  represents the scattering potential. We assume  $V(x, y)$  to be non-zero only within a finite region small compared to the width of the channel. We can now expand any stationary solution  $\psi_E(x, y)$  of the Schrödinger equation,  $H\psi_E(x, y) = E\psi_E(x, y)$ , in a Fourier series with  $x$ -dependent expansion coefficients using the complete set of transversal modes,

$$\psi_E(x, y) = \sum_{n=1}^{\infty} c_n(x) \chi_n(y), \quad (3)$$

where  $\chi_n(y)$  is the transverse state of the electron in the absence of the scatterer. Inserting this series into the Schrödinger equation and employing orthogonality of the transversal modes we obtain a set of coupled equations,

$$\frac{\partial^2}{\partial x^2} c_m(x) + k_m^2 c_m(x) = \sum_n M_{mn}(x) c_n(x), \quad (4)$$

with the definitions of the mode coupling constants  $M_{mn}(x)$  and the wave vector  $k_m$ ,

$$M_{mn}(x) = \frac{2m}{\hbar^2} \int dy \chi_m^*(y) V(x, y) \chi_n(y), \quad (5)$$

$$k_m = \sqrt{\frac{2m}{\hbar^2} (E - E_m)}. \quad (6)$$

Outside the scattering region the solution is given by linear combinations of the form

$$c_n(x) = \begin{cases} A_n e^{ik_n x} + B_n e^{-ik_n x} & x \ll 0 \\ C_n e^{ik_n x} + D_n e^{-ik_n x} & x \gg 0 \end{cases} \quad (7)$$

For  $k_n$  real, we get propagating modes, for  $k_n$  imaginary evanescent modes. By matching the wavefunctions for both regions with the appropriate boundary conditions, the coefficients for incoming and outgoing waves can be obtained.

The transmission coefficient for propagating modes is defined as  $T_{mn} = \frac{k_n}{k_m} \frac{|C_n|^2}{|A_m|^2}$  and the total transmission function as

$$T(E) = \sum_{mn \text{ (prop.)}} T_{mn} \quad (8)$$

where the sum extends over all propagating modes. The conductance is finally calculated using Eq. (1).

The transmission coefficients can also be obtained from the Green's function of the system. More specifically, it is the retarded Green's function that governs this behavior and via its poles also describes resonance behavior.<sup>3,13</sup> The retarded Green's function for the wire without scatterer is given by

$$G^0(x, y, x', y') = \sum_{n=1}^{\infty} \chi_n^*(y) \chi_n(y') \frac{2m}{\hbar^2} \frac{e^{ik_n |x-x'|}}{2ik_n} \quad (9)$$

or

$$G_{ab}^0(x, x') = \int dy dy' \chi_a^*(y) G^0(x, y, x', y') \chi_b(y') \propto \delta_{ab}. \quad (10)$$

The full solution can then be obtained from the Dyson equation

$$G_{ab}(x, x') = G_{ab}^0(x, x') + \sum_{c,d} \int dx'' G_{ac}^0(x, x'') V_{cd}(x'') G_{db}(x'', x') \quad (11)$$

with

$$V_{cd}(x'') = \int dy \chi_c^*(y) V(x'', y) \chi_d(y). \quad (12)$$

### III. SIMPLE MODEL SYSTEMS

We will now apply the general outline of the previous section to two simple model systems: the case of the  $\delta$ -function scatterer described by

$$V(x, y) = \gamma \delta(x) \delta(y - y_0) \quad (13)$$

and discussed by various authors,<sup>8,14,15</sup> as well as the slightly more realistic model with

$$V(x, y) = \gamma \delta(x) \frac{1}{\sqrt{\pi} \rho} \exp\left(-\frac{y^2}{\rho^2}\right) \quad (14)$$

describing a softer “impurity” scatterer in transversal direction.<sup>16</sup>

For both potentials, the waveguide can be split in two separate regions at  $x = 0$  and Eq. (7) can be written as

$$c_n(x) = \begin{cases} A_n e^{ik_n x} + B_n e^{-ik_n x} & x < 0 \\ C_n e^{ik_n x} + D_n e^{-ik_n x} & x > 0 \end{cases} \quad (15)$$

As  $\psi$  must be continuous at  $x = 0$  and its derivative must have a finite jump there, the same conditions must hold for the expansion coefficients  $c_n(x)$ . Thus using these two conditions on Eq. (4) with the ansatz in Eq. (15) yields

$$A_n + B_n = C_n + D_n, \quad (16)$$

$$ik_n (C_n - D_n) - ik_n (A_n - B_n) = \sum_m M_{nm} (A_m + B_m). \quad (17)$$

If  $\psi$  is an evanescent mode, we can set  $k_n = i\kappa_n$  and must require  $A_n = 0$  and  $D_n = 0$  to have a normalizable wavefunction. The coupling constants are given by

$$M_{nm} = \frac{2m\gamma}{\hbar^2} \chi_n^*(y_0) \chi_m(y_0) \quad (18)$$

for the case of the  $\delta$ -function scatterer, Eq. (13), and

$$M_{nm} = \frac{2m\gamma}{\hbar^2} \int dy \chi_m^*(y) \frac{1}{\sqrt{\pi} \rho} \exp\left(-\frac{y^2}{\rho^2}\right) \chi_n(y) \quad (19)$$

for the “impurity” scatterer, Eq. (14). In either case, the coupling constants do not depend on  $x$  anymore. For given coupling constants  $M_{nm}$ , the transmission coefficients can be computed by solving Eqs. (16) and (17). For an attractive potential ( $\gamma < 0$ ) resonance dips can be observed just below the energy at which a new propagating mode develops. Their position and width depends sensitively on the number of modes and the scatterer's strength.<sup>15</sup>

We note that in the case of the  $\delta$ -function scatterer, the integral equation for the full Green's function, Eq. (11), can be solved explicitly to yield<sup>14</sup>

$$G(x, y, x', y') = G^0(x, y, x', y') + \frac{G^0(x, y, 0, y_0) G^0(0, y_0, x', y')}{1/\gamma - G^0(0, y_0, 0, y_0)}. \quad (20)$$

We first briefly summarize the results for the  $\delta$ -function scatterer. As there is no solution to a two-dimensional  $\delta$ -function the problem would be ill-posed unless one restricts the problem to a finite number of transverse modes. The potential is then equivalent to an  $s$ -like scatterer. As more modes are included the electron becomes more strongly localized. For the following computations, we will use the parameters  $D = 300 \text{ \AA}$  for the width of the channel (hard wall potential),  $y_0 = \frac{5}{12}D$  for the transversal position of the scatterer, and the mass  $m = 0.067m_e$  as the effective mass of an electron in GaAs-AlGaAs heterostructures. The total number of modes will be denoted by  $n_c$ . For a potential strength of  $\gamma = \mp 7 \text{ feV cm}^2$ , the resulting conductance is shown in Figs. VII (dashed line) and VII (dotted line). The dependence of the pole location on the number of modes can be seen in Fig. 3 (dots), with no indication of convergence with respect to  $n_c$ .

This convergence problem can be avoided by modifying the  $\delta$ -function potential in  $y$ -direction to the smoother form of a Gaussian function as in Eq. (14). The finite width allows the higher modes to decouple from the lower ones. In the limit  $\rho \rightarrow 0$ , we recover the  $\delta$ -function potential with the potential strength  $\gamma$ . By numerically evaluating the integrals for the coupling constants, Eq. (19), one can again obtain the full transmission function and thus the conductance. As expected, the conductance curves closely resembles the results for the  $\delta$ -function scatterer, showing the same characteristic resonance dip for attractive scatterers. Numerical results for the exact pole location of the transmission function are shown in Fig. 4 using the potential parameters  $\gamma = -7 \text{ feV cm}^2$  and  $\rho = 3.0 \text{ \AA}$ . In contrast to the  $\delta$ -function potential, the result converges to its exact solution when using a large enough, but finite number of modes.

Nevertheless, the characteristic behavior of the conductance is identical to the  $\delta$ -function scatterer with a finite number of modes. This again demonstrates that the  $\delta$ -function scatterer serves its purpose as a useful model if it is interpreted as an  $s$ -like scatterer for a fixed finite number of modes.

#### IV. SCALING APPROACH

The methods presented in the last section work fine except that they require an infinite or very large (for a strongly localized scatterer) number of modes to be included. Simply cutting of the sum at some small number does not give the correct answer. But calculations for

large  $n_c$  have the drawback that substantial computing power is needed. Therefore it would be useful if one could find a way to reduce the number of modes in the calculation without neglecting their influence. A well known technique for this kind of problem is the poor man's scaling approach.<sup>17</sup> The idea is the following: Consider a typical relevant process which includes an intermediate virtual state. The sum over the virtual states shall have a cut-off. If the system exhibits scaling behavior one can infinitesimally reduce the cut-off and incorporate the change into a new effective coupling constant for a process not involving these virtual states. By repeating these steps one can integrate out a large portion of the states.

For the present system this means that we investigate the influence of decreasing the mode cut-off  $n_c$  on the coupling constant  $\gamma$ .<sup>18</sup> In the spirit of poor man's scaling in the Kondo problem we look at a diagram as shown in Fig. 5 which represents a typical process in the wire. We will first discuss this in terms of a general scatterer before we show the detailed calculation for the  $\delta$ -function scatterer from above. The contribution of the diagram is given by

$$\sum_{c=1}^{n_c} \int dx'' dx''' G_{aa}^0(x, x'') V_{ac}(x'') G_{cc}^0(x'', x''') \times V_{cb}(x''') G_{bb}^0(x''', x'). \quad (21)$$

The cut-off  $n_c$  stops the summation of the intermediate modes. Reducing the cut-off by one mode amounts to a difference that equals the  $n_c$ 's summand. This change should be incorporated into the new coupling constant that is taken for a process with only one scattering event, which would have the following form

$$\int dx'' G_{aa}^0(x, x'') V'_{ab}(x'') G_{bb}^0(x'', x') \quad (22)$$

where the  $V'_{ab}(x'')$  denotes a potential with renormalized coupling constant. Assuming that although  $n_c$  is clearly integer we can treat the difference as infinitesimal, and that the potential can always be written as  $V_{ab}(x) = \gamma \tilde{V}_{ab}(x)$ , we can formally write

$$\frac{\delta\gamma}{\delta n_c} = - \left( \tilde{V}_{ab}(x'') \right)^{-1} \times \int dx''' V_{an_c}(x'') G_{n_c n_c}^0(x'', x''') V_{n_c b}(x'''). \quad (23)$$

This equation is in general difficult to solve, and could potentially contain an explicit dependence on  $a$  and  $b$ .<sup>19</sup> We therefore show how to solve this equation for the  $\delta$ -function scatterer with a finite number of modes as discussed above. The contribution of the diagram is given by  $\gamma G_{n_c n_c}^0(0, 0) \gamma$ . For large  $n_c$  we can thus write the change in  $\gamma$  as

$$\frac{\delta\gamma}{\delta n_c} = -\gamma^2 \frac{2}{D} \frac{2m}{\hbar^2} \sin^2 \left( \frac{\pi n_c y_0}{D} \right) \frac{1}{2ik_{n_c}}. \quad (24)$$

For large  $n_c$  we can approximate  $k_{n_c} \approx \frac{in_c\pi}{D}$  and integrate Eq. (24) to obtain

$$-\frac{1}{\gamma} = \frac{2m}{\hbar^2\pi} \left( -\frac{1}{2} \text{Ci} \left( \frac{2\pi y_0 n_c}{D} \right) + \frac{1}{2} \ln n_c \right) + \text{const.} \\ \cong \frac{m}{\hbar^2\pi} \ln n_c + \text{const.}, \quad (25)$$

where the last equality holds again for large  $n_c$  and  $\text{Ci}(x)$  is the integral cosine function. Since we expect a small change of the cut-off not to change the result as a whole we can deduce the renormalization group equation

$$n_c \exp \left( \frac{\hbar^2\pi}{m\gamma} \right) = \tilde{n}_c \exp \left( \frac{\hbar^2\pi}{m\tilde{\gamma}} \right). \quad (26)$$

With the help of Eq. (26) we can now calculate the conductance for a model with a large number of modes  $n_c$  by including only  $\tilde{n}_c$  modes and the renormalized coupling

$$\tilde{\gamma} = \frac{1}{\frac{1}{\gamma} + \frac{m}{\hbar^2\pi} \ln \frac{n_c}{\tilde{n}_c}}. \quad (27)$$

The cut-off  $\tilde{n}_c$  must be chosen such that the approximations made above are valid, i. e. the renormalization procedure will eventually break down for small  $\tilde{n}_c$ . Moreover, there is one strict physical criterion for a minimum lower bound to  $\tilde{n}_c$ : To reproduce the resonance behavior of the full system, it is at least necessary to include one evanescent mode in the renormalized calculation.<sup>15</sup> We would also like to point out that a divergence of  $\tilde{\gamma}$  is not only possible in Eq. (27), but furthermore that it may even abruptly change sign from  $-\infty$  to  $+\infty$ . This is however not problematic: As can be seen from Eq. (20) it is  $1/\gamma$  that enters the Green's function, telling us that  $\gamma \rightarrow \pm\infty$  show the same physics, independently of the sign of the coupling strength. With increasing scatterer strength, the transmittive behavior of the attractive scatterer indeed more and more resembles that of the repulsive scatterer.<sup>8</sup>

## V. COMPARISON TO EXACT FORMALISM

In this section we show and compare the results when the formalism from above is applied to the single  $\delta$ -function scatterer given by Eq. (13). At the end we discuss the implications of this scaling behavior. In Fig. VII we show the conductance of a system with an attractive (top) and a repulsive (bottom)  $\delta$ -function scatterer with a finite number of modes. The shape of the curves is altered by a variation of  $n_c$ , especially the width and position of the resonance in the attractive case are quite sensitive (comparing e. g. the dotted and dashed lines). When we apply the scaling approach, Eq. (27) to the model with  $n_c = 100$  and scale it down to  $\tilde{n}_c = 10$ , we obtain an almost identical result (solid line). This clearly confirms the validity of our approach. In Fig. VII we

again plot the conductance for the attractive case. This time we scale down to  $\tilde{n}_c = 50, 10$ , and  $5$ . For large  $\tilde{n}_c$  the method works very well, but as we get to small values of  $\tilde{n}_c$ , it eventually breaks down. However we used the assumption that  $n_c$  is large in our derivation, so this breakdown is expected. But even for  $\tilde{n}_c = 5$  it still gives fairly good results. Another limit is reached when the number of propagating modes is close to  $\tilde{n}_c$ . But only for  $n_{\text{prop}} \geq \tilde{n}_c$  it breaks down completely, as there is no evanescent mode left which could build up the resonance. It may seem surprising that such a simple method yields these results. However, it confirms that the type of process we have chosen is indeed the relevant one.

An alternative description of resonance behavior can be given in terms of quasi-bound state. They are defined as the poles of the energy Green's function in the complex energy plane. Hence our approach should apply to the quantities of this approach as well. In Fig. 3 we show that the location of the poles can be calculated very well with the scaling method. It is remarkable that even down to  $n_c = 2$ , all poles lie very close to the correct value. Moreover, they are not randomly scattered around  $n_c = 100$ , but rather lie on the parabolic curve of the poles for increasing  $n_c$ .

Our result shows that although a true description of quantum wires with scatterers requires the inclusion of all modes, the presence of higher modes does not have a strong affect on the low energy behavior. Their influence can be cast in a renormalized value of the coupling constant. Therefore one can say that calculations done on these waveguide systems with a few number of modes should give qualitatively correct results. This is not a trivial result, because the mechanism of the suppression of the higher modes is not of thermal origin. Rather it is the scaling behavior of these systems that allows our conclusion.

## VI. MANY SCATTERER CASE

Another important consequence is that future calculations need to be done only for a few low lying modes. This is important especially for systems with many scatterers: Due to the scattering matrix multiplication, the computing time grows linearly with the number of scatterers and grows more than quadratic with the number of modes. When choosing  $\tilde{n}_c$  one needs of course to make sure, that the evanescent modes are strongly enough localized, such that they do not carry a virtual current<sup>20</sup> and thereby provide a minimum upper cut-off. In order to demonstrate this, we perform a calculation for the simple case of two  $\delta$ -function scatterers placed in series and separated by a distance  $d$ . For a few number of modes this model has been discussed in Reference 21. Here we present results for the case of many modes and discuss how they can be obtained using our scaling method.

The specific system under consideration consists of two

$\delta$ -function scatterers located at  $(0, y_1)$  and  $(d, y_2)$ , with potential strengths  $\gamma_1$  and  $\gamma_2$  respectively. The waveguide itself shall be the same as before. The Green's function of this system can be obtained analytically and is given by the lengthy, however very useful expression

$$G(x, y, x', y') = G^0(x, y, x', y') + \gamma_1 G^0(x, y, 0, y_1) \frac{c_1 + a_1 c_2}{1 - a_1 a_2} + \gamma_2 G^0(x, y, d, y_2) \frac{c_2 + a_2 c_1}{1 - a_1 a_2} \quad (28)$$

where the following abbreviations have been used:

$$\begin{aligned} c_1 &= \frac{G^0(0, y_1, x', y')}{1 - \gamma_1 G^0(0, y_1, 0, y_1)}, \\ c_2 &= \frac{G^0(d, y_2, x', y')}{1 - \gamma_2 G^0(d, y_2, d, y_2)}, \\ a_1 &= \frac{\gamma_2 G^0(0, y_1, d, y_2)}{1 - \gamma_1 G^0(0, y_1, 0, y_1)}, \\ a_2 &= \frac{\gamma_1 G^0(d, y_2, 0, y_1)}{1 - \gamma_1 G^0(d, y_2, d, y_2)}. \end{aligned} \quad (29)$$

To apply our scaling method, we employ the approximation that the evanescent modes fall off exponentially. Hence contributions to the scaling of order  $\gamma_1 \gamma_2$  are strongly suppressed for higher modes, i. e.  $|k_n d|$  is large. We can then simply use the single scatterer result and apply it independently to both coupling constants. The results are shown in Fig. VII a) and b).

In Fig. VII a) we compare the conductance for various number of modes. Already for two modes the peaks in the lowest subband with one evanescent mode are present. The inclusion of higher modes however leads to a strong shift in position and shape. Although the true peak structure becomes visible for  $n_c = 10$ , it is fully developed only for many more modes. In addition, the results in the second subband are completely wrong for two modes. This should be expected since no evanescent mode is present. In Fig. VII b) we compare our scaling result to the exact one and again find that it works very well. It is remarkable that already for two modes the deviation in the first subband is negligible.

The generalization to many scatterers is obvious: one only has to keep in mind to take enough evanescent modes to mimic the decaying currents between the scatterers. The Fabry-Perot behavior that causes the oscillations is created by the propagating modes, however it can be enhanced by the first few evanescent ones.

## VII. CONCLUSION

In this article we discussed the conductance properties of ballistic quantum wires containing impurities. As shown, they depend strongly on the number of modes included and the calculations can thus become quite difficult. We proved that it is possible to incorporate the

effect of higher modes into an effective coupling constant for the lower lying modes. This was done by a poor man's scaling approach. For the  $\delta$ -function scatterer with a fixed number of modes we compared our result to exact calculations and found very good agreement. We therefore conclude that our approach does not only allow for quicker calculations but also shows that the system's behavior is governed by a few low-lying modes.

## ACKNOWLEDGMENTS

We thank Herbert Schoeller and Michele Governale for useful discussions. D. B. acknowledges financial support from the DFG Graduiertenkolleg 284: "Kollektive Phänomene im Festkörper". L. E. R. acknowledges partial support from Welch Foundation Grant No. 1052 and U.S. DOE Grant No. DE-FG03-94ER14405.

- 
- <sup>1</sup> R. Landauer, IBM J. Res. Dev. **1**, 223 (1957).
  - <sup>2</sup> M. Büttiker, IBM J. Res. Dev. **32**, 306 (1988).
  - <sup>3</sup> D. S. Fisher and P. A. Lee, Phys. Rev. B **23**, 6851 (1981).
  - <sup>4</sup> A. D. Stone and A. Szafer, IBM J. Res. Develop. **32**, 384 (1988).
  - <sup>5</sup> H. U. Baranger and A. D. Stone, Phys. Rev. B **40**, 8169 (1989).
  - <sup>6</sup> C.-T. Liang, M. Y. Simmons, C. G. Smith, D. A. Ritchie and M. Pepper, Appl. Phys. Lett. **75**, 2975 (1999).
  - <sup>7</sup> S. Datta, M. Cahay, and M. McLennan, Phys. Rev. B **36**, 5655 (1987).
  - <sup>8</sup> P. F. Bagwell, Phys. Rev. B **41**, 10354 (1990).
  - <sup>9</sup> P. F. Bagwell and R. K. Lake, Phys. Rev. B **46**, 15329 (1992).
  - <sup>10</sup> Y. B. Levinson, M. I. Lubin and E. V. Sukhorukov, Phys. Rev. B **45** 11936 (1992).
  - <sup>11</sup> C. Kunze and R. Lenk, Solid State Comm. **84**, 457 (1992).
  - <sup>12</sup> J. Wang, Q. Zheng, and H. Guo, Phys. Rev. B **55**, 9770 (1997).
  - <sup>13</sup> J. R. Taylor, *Scattering Theory: The Quantum Theory on Nonrelativistic Collisions* (John Wiley & Sons, New York, 1972).
  - <sup>14</sup> P. F. Bagwell, J. Phys.: Condens. Matter **2**, 6179 (1990).
  - <sup>15</sup> D. Boese, M. Lischka and L. E. Reichl, Phys. Rev. B **61**, 5632 (2000).
  - <sup>16</sup> M. Y. Azbel, Phys. Rev. B **43**, 6717 (1991); E. Granot, Phys. Rev. B **60**, 10664 (1999).
  - <sup>17</sup> P. W. Anderson, J. Phys. C, **3**, 2436 (1970).
  - <sup>18</sup> Regardless of the scattering potential,  $V(x, y)$  can always be cast in a form such that it is proportional to a coupling constant  $\gamma$ .
  - <sup>19</sup> The explicit  $a$  and  $b$  dependence can in principle be treated by carrying them along all the way. This however would lead to a serious complication of the scaling and the conductance calculations.

<sup>20</sup> We refer to a virtual current as an evanescent mode that decays from one scatterer but 'reaches' the other scatterer and therefore can carry a current.

<sup>21</sup> A. Kumar and P. F. Bagwell, Solid State Comm. **75**, 949 (1990); Phys. Rev. B **43** 9012 (1991); *ibid.* **44** 1747 (1991).

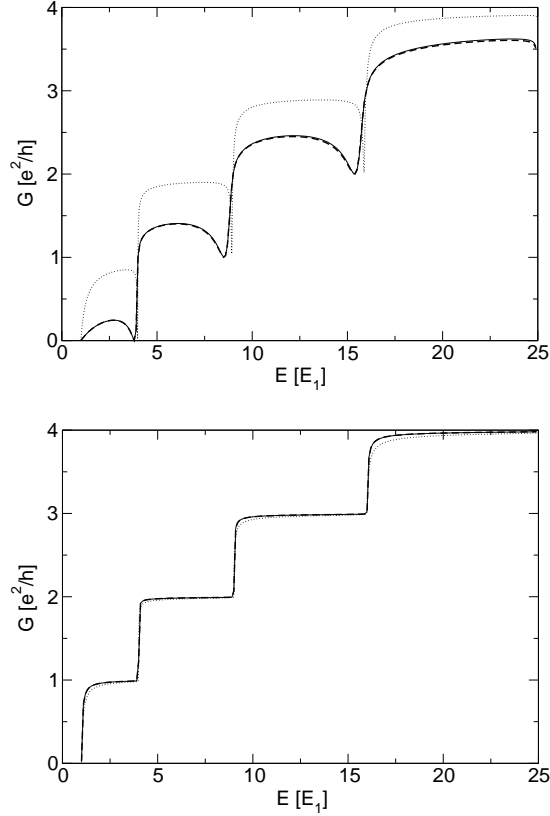


FIG. 1. The conductance for an attractive (top) and a repulsive (bottom)  $\delta$ -scatterer of strength  $\gamma = \mp 7 \text{ feV cm}^2$  and  $n_c = 100$  (dashed),  $n_c = 10$  (dotted) and  $n_c = 100$  scaled down to  $\tilde{n}_c = 10$  (solid). The original curve with  $n_c = 100$  and the rescaled one with  $\tilde{n}_c = 10$  lie nearly on top of each other.

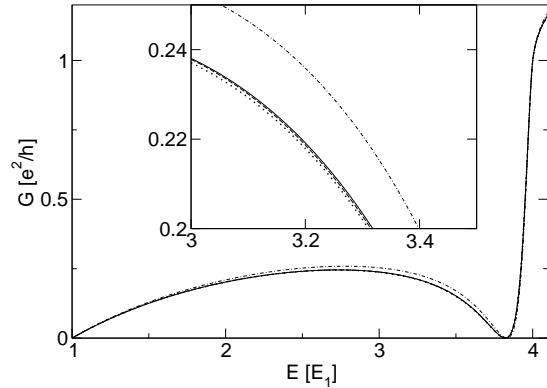


FIG. 2. The conductance for an attractive  $\delta$ -scatterer of strength  $\gamma = -7 \text{ feV cm}^2$ ,  $n_c = 100$  calculated without scaling (dotted) and with  $\tilde{n}_c$  rescaled to 10 (solid), to 50 (dashed), and to 5 (dot-dashed). If the number of modes after the scaling is large enough, the difference is hardly visible.

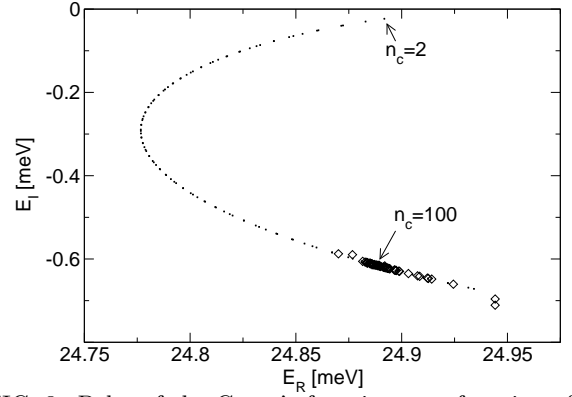


FIG. 3. Poles of the Green's function as a function of  $n_c$ . The dots indicate the pole location for values from  $n_c = 2$  to  $n_c = 110$ . The diamonds represent the case  $n_c = 100$  with  $\tilde{n}_c$  varying between 2 and 60.

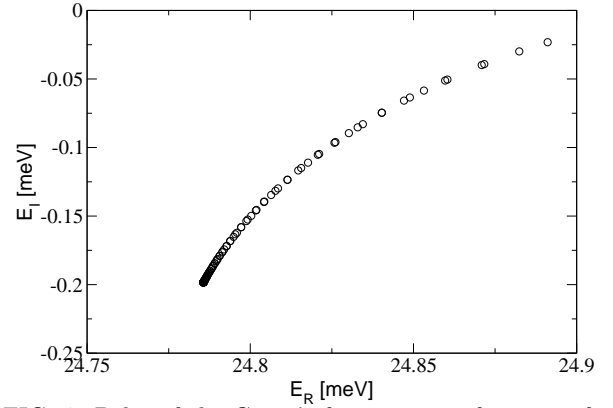


FIG. 4. Poles of the Green's function as a function of  $\tilde{n}_c$ . The circles indicate the pole location for values from  $n_c = 2$  to  $n_c = 110$ . When using  $n_c = 80$  modes, the pole location is converged to its final position.

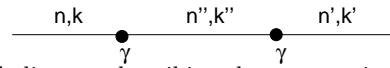


FIG. 5. A diagram describing the propagation from a state characterized by mode  $n$  and longitudinal momentum  $k$  via two scattering events into the state  $n', k'$ .

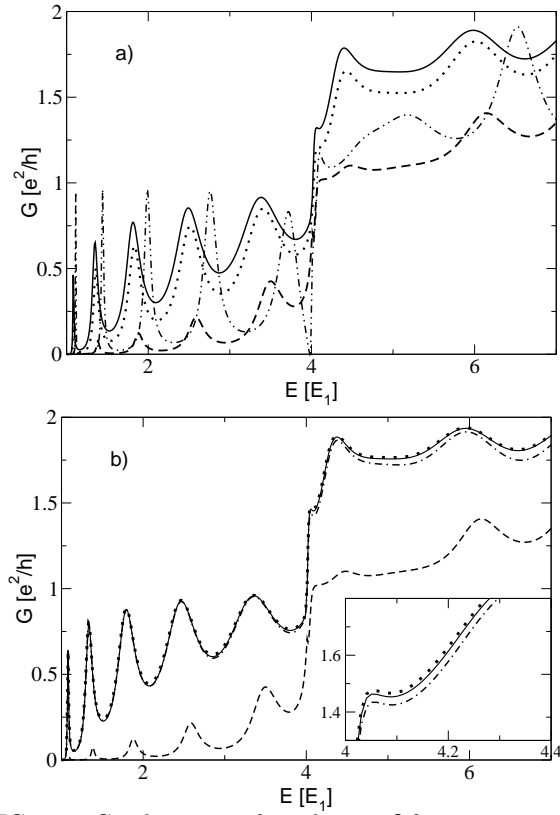


FIG. 6. Conductance for the 2  $\delta$ -function scatterer case. The used parameter values are  $\gamma_1 = 25 \text{ feV cm}^2$ ,  $\gamma_2 = -25 \text{ feV cm}^2$  and  $d = 90 \text{ nm}$ . In a) the different lines are  $n_c = 50$  (solid), 30 (dotted), 10 (dashed) and 2 (dot-dashed). One can see that already from  $n_c = 10$  on, the qualitative behavior is the same.

In b) the scaling is applied to the  $n_c = 100$  case (solid) and performed down to  $\tilde{n}_c = 10$  (dotted) and 2 modes (dot-dashed). The dashed line shows how well it compares to the case with  $n_c = 10$  modes without scaling.